PREPRINT NUMBERS HERE manuscript No.
(will be inserted by the editor)

Precise predictions for same-sign W-bosons scattering at the LHC

Benedikt Biedermann[1], Simon Brass[2], Ansgar Denner[1], Stefan Dittmaier[3], Pietro Govoni[4], Michele Grossi[5,6], Alexander Karlberg[7], Mathieu Pellen[1], Giovanni Pelliccioli[8], Simon Plätzer[9], Michael Rauch[10], Jürgen Reuter[11], Vincent Rothe[11], Christopher Schwan[3], Pascal Stienemeier[11], Marco Zaro[12]

[1]Universität Würzburg, Institut für Theoretische Physik und Astrophysik, Emil-Hilb-Weg 22, 97074 Würzburg, Germany
[2]Universität Siegen, Department Physik, Walter-Flex-Str.3, 57068 Siegen, Germany
[3]Albert-Ludwigs-Universität Freiburg, Physikalisches Institut, Hermann-Herder-Str. 3, 79104 Freiburg, Germany
[4]Milan, Italy
[5]Universitá di Pavia, Dipartimento di Fisica and INFN, Sezione di Pavia, Via A. Bassi 6, 27100 Pavia, Italy
[6]IBM Italia s.p.a. Circonvallazione Idroscalo , 20090 Segrate (MI), Italy
[7]Department of Physics, University of Zürich, CH-8057 Zürich, Switzerland
[8]Università di Torino, Dipartimento di Fisica and INFN, Sezione di Torino, Via P. Giuria 1, 10125 Torino, Italy
[9]Particle Physics, Faculty of Physics, University of Vienna, Vienna, Austria
[10]Institute for Theoretical Physics, Karlsruhe Institute of Technology (KIT), Karlsruhe, Germany
[11]DESY Theory Group, Notkestr. 85, D-22607 Hamburg, Germany
[12]Nikhef, Science Park 105, 1098XG Amsterdam, The Netherlands
the date of receipt and acceptance should be inserted later

Abstract

In this article, a detailed study of the vector-boson scattering for two positively charged W bosons is presented. In particular, a comparison between the full next-to-leading (NLO) QCD corrections against several approximations is carried out. This study is not only performed in the usual fiducial region used by experimental collaborations but also in a more inclusive set-up. This allows to infer precisely the quality of such approximations. Finally, NLO predictions matched to various parton shower are discussed. This study allows thus to infer the systematic errors related to vector-boson scattering at the NLO-QCD level and beyond.

1 Introduction

Vector-boson scattering (VBS) is a class of processes that allow to probe the nature of Higgs-vector-vector couplings and quartic gauge couplings. It is usually understood that VBS refers to the scattering of massive vector-bosons ($W^{\pm}, Z$), which therefore couple to the Higgs and can be longitudinally polarized. The scattering of longitudinally polarized bosons is of particular interest, because the corresponding matrix elements feature both gauge- and unitarity cancellations that strongly depend on the actual form of the Higgs-sector. A detailed study of this class of processes will therefore further constrain the Higgs-couplings and hint at or exclude non-Standard Model Higgs bosons.

The process with two positively charged W bosons is the VBS process with the largest signal-background ratio at the LHC, for which evidence has been found in 8 TeV data [1, 2] and which is now started to be observed [3] and measured [4] in 13 TeV data. For now the measurements of VBS processes are limited by statistics but the situation will change in a near future. On the theoretical side, it is thus of prime importance to provide precise predictions and infer their related systematic errors.

The W^+W^+ scattering is the simplest VBS process to calculate, because the double-charge structure of the leptonic final state limits the number of partonic processes and total number of Feynman diagrams for each process. It also implies that irreducible backgrounds are

comparatively small, which make this VBS process experimentally favourable in comparison to e.g. W^+W^- scattering, which has the largest cross section. Therefore, it is an ideal candidate for a detailed study of various theoretical predictions.

In the last few years, several leading order (LO) and next-to-leading order (NLO) computations became available for both the VBS process [5–8] and its QCD-induced irreducible background process [8–12]. These computations all rely on approximations, while recently the complete NLO corrections have been performed [13]. It is therefore interesting to infer in details the quality of the various approximations. Indeed, apart from Ref. [13] where it is commented on, [MP: more references?] no detailed comparison of the VBS approximations have been carried out. Preliminary results have already been made public in Ref. [proceedings Split].

The hadronic process is $pp \to \mu^+\nu_\mu e^+\nu_e jj + X$, which includes the W^+W^+ scattering. This final state possesses three contributions at LO whose coupling orders are $\mathcal{O}(\alpha^6)$, $\mathcal{O}(\alpha_s\alpha^5)$, and $\mathcal{O}(\alpha_s^2\alpha^4)$. They are commonly referred to as electroweak (EW), interference, and QCD contributions, respectively.[1] Therefore, the present work starts with a LO study of these three contributions as a function of typical VBS cuts. This allows to identify the various contributions to the final state $\mu^+\nu_\mu e^+\nu_e jj$. This is followed by a LO comparison between the various predictions at the level of the cross section and differential distributions.

At NLO, the process possesses four contributions of orders $\mathcal{O}(\alpha^7)$, $\mathcal{O}(\alpha_s\alpha^6)$, $\mathcal{O}(\alpha_s^2\alpha^5)$, and $\mathcal{O}(\alpha_s^3\alpha^4)$. The largest one are the EW corrections [13, 14] of order $\mathcal{O}(\alpha^7)$. The contribution to the order $\mathcal{O}(\alpha_s\alpha^6)$ is the second largest NLO contribution and is often referred to as the QCD corrections to the VBS process. In the following, this order is the one where our comparisons are focused on; in this article we will refer to it as simply NLO. As for the LO study, the various predictions are compared at the level of the cross section and differential distributions. In particular, this allows to infer the accuracy of the so-called VBS approximation, which we will define in more detail later. To our knowledge, such a detailed study was still missing.

Finally, several predictions featuring parton shower are compared. This allows to infer systematic differences between the various predictions. This is the first time in the literature that such an analysis has been carried out [MP: True?] .

Obviously all VBS processes deserve such a study but the present article sets the standard for inferring systematics related to NLO corrections and beyond.

[1] The EW contribution is sometimes referred to as the VBS contribution even it possesses non-VBS contributions.

The article is organised as follow: In Sec. 2 the studied process is defined. Various approximation at LO and NLO are described in Sec. 3. This is followed by a presentation of the programs used for the computations. Sections 4 and 5 are devoted to a LO and NLO study, respectively. Section 6 deals with the matching to parton shower. The last section consists in concluding remarks and recommendations for experimental collaborations.

2 Definition of the process

The scattering of two positively charged W bosons is proceeding at the LHC through the partonic process:

$$pp \to \mu^+\nu_\mu e^+\nu_e jj + X. \tag{1}$$

This process possesses three LO contributions of different orders. The first one is of order $\mathcal{O}(\alpha^6)$ is referred to as EW contributions. In addition to typical VBS contributions as shown on the left of Fig. 1, it also features s-channel contributions. These types of contributions will play a particular role in the study of the various contributions in Section 4.1. Some of them take the form of decay chains as for example the diagram represented in the middle of Fig. 1 while others are tri-boson contributions (right of Fig. 1). The VBS diagrams typically dominate the full process. But all these contributions form a single gauge-invariant set of contributions and therefore cannot be separated.

The process can also be mediated via a gluon connecting the two quark lines while the W bosons are radiated from the quark lines. These contributions are of order $\mathcal{O}(\alpha_s^2\alpha^4)$ and usually feature different kinematic behaviours than the EW contribution. Nonetheless they share the same final state and therefore constitute an irreducible background.

Finally, due to the specific colour structure of these two classes of amplitudes, there exist non-zero interferences. These are of order $\mathcal{O}(\alpha_s\alpha^5)$ and are usually small but not negligible for realistic experimental set-ups [13].

Usually, in experimental measurements, special VBS-cuts are designed in order to enhance the EW contribution over the QCD one. These cuts are based on the fact that the two contributions have rather different kinematic. The EW contribution is characterised by two jets with large rapidity in the peripheral region as well as a large invariant mass. The two W bosons are mostly produced centrally. This is in opposition with the QCD component which favours jets in the central region. Therefore, the event selection usually involves rapidity-difference and invariance mass cuts for the jets. This will also be discussed in Section 4.1.

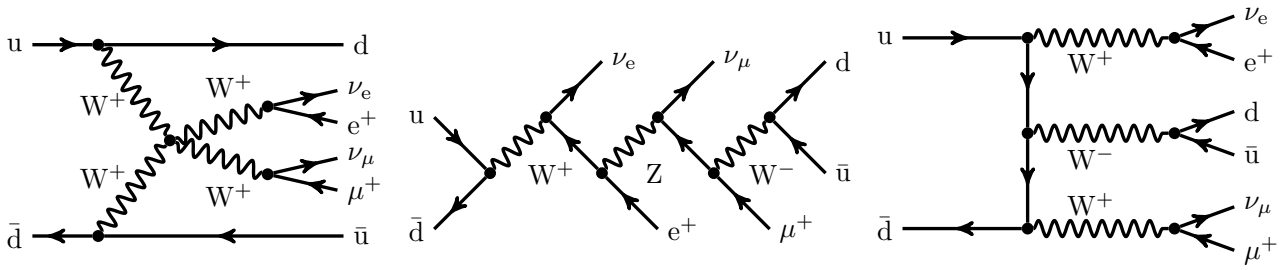

Fig. 1: Sample tree-level diagrams that contribute to the process pp $\to \mu^+\nu_\mu e^+\nu_e jj$ at order $\mathcal{O}(\alpha^6)$. In addition to typical VBS contribution (left), this order also possesses s-channel (middle) and tri-boson contributions (right).

3 Details of the calculations

3.1 Several descriptions for one process

As mentioned previously, the EW contribution is dominated by the scattering of two W gauge bosons. Therefore it is justified to approximate the full EW contributions simply by the VBS contributions. Nonetheless, this set of contributions is not gauge invariant. To make it gauge-invariant, one should project on-shell the incoming W boson. Unfortunately, this momentum is space-like and thus a simple on-shell projection is not possible. Instead, one can keep the W boson leg connected to the external quark line off-shell while the one connected to the scattering is put on-shell. Then the polarisation of the gauge boson is accommodated following the implementations of Refs. [15, 16]. Such an approximation is usually called effective vector-boson approximation (EVBA).

A more refined approximation consists in considering all t- and u- diagrams and square them separately. Nonetheless, different type of diagrams are not squared which amounts to neglecting interferences. These interferences are expected to be small in the VBS fiducial region. The s-channel contributions can still be left out. This approximation is often called t-/u- approximation or even VBS approximation. We will adopt the latter denomination in the following of the article. Such an approximation is implemented at LO in the computer codes Bonsay and Powheg. The physical origin of this approximation is that each proton emitting a quark represents two independent copies of the $SU_c(3)$ gauge group.

The squared matrix element of the s-channel contributions can then be added but all interferences between different kinematic channels are neglected. This is what is done in VBFNLO.

All other codes (MG5_aMC, MoCaNLO+Recola, PHANTOM, and Whizard) consider all contributions of order $\mathcal{O}(\alpha^6)$ as well as all possible interferences. Note that the final W boson can always be considered either on-shell or off-shell without affecting the previous discussion. All the codes mentioned here are described in details in the following sub-section.

Moving on to NLO accuracy, one can extend the approximation presented at LO. The VBS approximation at NLO is simply extending the same approximation to real as well as to virtual corrections. This is implemented in POWHEG. This approximation can be used in combination with a double-pole approximation [REF] for the virtual contribution. This requires the computation of factorisable as well as non-factorisable corrections [17] separately. Such an approximation is implemented in Bonsay. In VBFNLO, the VBS approximation at NLO with s-channel contributions is implemented.

A further refinement is to consider the full real contributions as well as part of the virtual [MP: I cannot remember exactly what is included] . This assumes a cancellation of infrared poles. Such predictions are provided by MG5_aMC.

Finally the full computation implies to also consider EW corrections in the virtual as well as real corrections [13]. Such full predictions are provided by the combination MoCaNLO+Recola as published in Ref. [13].

In Tab. 1 the details of the various codes are reported. In particular, it is specified whether

- all s- and t/u-channel diagrams that lead to the considered final state are included;
- interferences between diagrams are included at LO;
- diagrams which do not feature two resonant vector bosons are included;
- the so-called non-factorisable (NF) QCD corrections, that is the corrections where (real or virtual) gluons are exchanged between different quark lines, are included;
- EW corrections to the $\mathcal{O}(\alpha^5\alpha_s)$ interference are included. These corrections are of the same order as the NLO QCD corrections to the $\mathcal{O}(\alpha^6)$ term.

Code	$\mathcal{O}(\alpha^6)$ $\lvert s\rvert^2$/ $\lvert t\rvert^2$/$\lvert u\rvert^2$	$\mathcal{O}(\alpha^6)$ interf.	Non-res.	NLO	NF QCD	EW corr. to $\mathcal{O}(\alpha_s\alpha^5)$
Bonsay	t/u	No	Yes, virt. No	Yes	No	No
POWHEG	t/u	No	Yes	Yes	No	No
MG5_aMC	Yes	Yes	Yes	Yes	No virt.	No
MoCaNLO+Recola	Yes	Yes	Yes	Yes	Yes	Yes
PHANTOM	Yes	Yes	Yes	No	-	-
VBFNLO	Yes	No	Yes	Yes	No	No
Whizard	Yes	Yes	Yes	No	-	-

Table 1: Summary of the different properties of the codes employed in the comparison.

3.2 Description of the predictions

In the comparison, the following codes are used:

- The program Bonsay consists of a general-purpose Monte Carlo integrator and matrix elements taken from several sources: Born matrix elements are adapted from the program Lusifer [18] for the partonic processes, real matrix elements are written by Marina Billoni, and virtual matrix elements by Stefan Dittmaier. One loop integrals are evaluated using the Collier library [19, 20].
- MadGraph5_aMC@NLO [21] is an automatic meta-code (a code that generates codes) which makes it possible to simulate any scattering process including NLO QCD corrections both at fixed order and including matching to parton showers. It makes use of the FKS subtraction method [22, 23] (automated in the module MadFKS [24, 25]) for regulating IR singularities. The computations of one-loop amplitudes are carried out by switching dynamically between two integral-reduction techniques, OPP [26] or Laurent-series expansion [27], and TIR [28–30]. These have been automated in the module MadLoop [31], which in turn exploits CutTools [32], Ninja [33, 34], or IREGI [35], together with an in-house implementation of the OpenLoops optimisation [36].
  The simulation of VBS at NLO-QCD accuracy can be performed by issuing the following commands in the program interface:

  ```
  > set complex_mass_scheme #1
  > import model loop_qcd_qed_sm_Gmu #2
  > generate p p > e+ ve mu+ vm j j QCD=0 [QCD] #3
  > output #4
  ```

  With these commands the complex-mass scheme is turned on #1, then the NLO-capable model is loaded #2[2], finally the process code is generated #3 (note the QCD=0 syntax to select the purely-electroweak process) and written to disk #4. Because of some internal limitations, which will be lifted in the future version capable of computing both QCD and EW corrections, only loops with QCD-interacting particles are generated. [MP: Detail of the approximation done, divergent part, assumed to cancel etc.]
- Phantom [37] is a dedicated tree–level Monte Carlo for six parton final states at pp, $p\bar{p}$ and e^+e^- colliders at α^6 and $\alpha^4\alpha_s^2$ including interferences between the two sets of diagrams. It employs complete tree–level matrix elements in the complex–mass scheme [38] computed via the modular helicity formalism [39, 40]. The integration uses a multichannel approach [41] and an adaptive strategy [42]. Phantom generates unweighted events at parton–level for both the SM and a few instances of BSM theories.
- The Powheg-Box [43, 44] is a framework for matching NLO-QCD calculations with parton showers. It relies on the user providing the matrix elements and Born phase space, but will automaticaly construct FKS [22] subtraction terms and the phase space for the real emission. For the VBS processes all matrix elements are being provided by a previous version of VBFNLO [45, 46, 12] and hence the approximations used in the Powheg-Box are the similar to those used in VBFNLO. [MP: Mention the non-clustering for the scale as well as the different running of alphas at NLO.]
- The program MoCaNLO+Recola is made of a flexible Monte Carlo program dubbed MoCaNLO [47] and the general matrix element generator Recola [48, 49]. To numerically evaluate the one-loop scalar and tensor integrals, Recola relies on the Collier library [19, 20], These tools have been successfully used for the computation of NLO corrections for VBS [14, 13].
- VBFNLO [45, 46, 12] is a flexible parton-level Monte Carlo for processes with electroweak bosons. It allows the calculation of VBS processes at NLO QCD in the VBF approximation and including the s-channel triboson contribution, neglecting interferences between the two. Besides the SM, also anomalous couplings of the Higgs and gauge bosons can be simulated.

[2] Despite the loop_qcd_qed_sm_Gmu model also includes NLO counterterms for computing electro-weak corrections, it is not yet possible to compute such corrections with the current version of the code.

– Whizard [50, 51] is a multi-purpose event generator with the LO matrix element generator O'Mega. It provides FKS subtraction terms for any NLO process, while virtual matrix elements are provided externally by OpenLoops [36] (alternatively, Recola [48, 49] (cf. above) can be used as well). Whizard allows to simulate a huge number of BSM models as well, in particular for new physics in the VBS channel in terms of both higher-dimensional operators as well as explicit resonances.

3.3 Input parameters

We simulate VBS production at the LHC, with a center-of-mass energy $\sqrt{s} = 13\,\text{TeV}$. We assume five massless flavours in the proton, and employ the NNPDF 3.0 parton density [52] with NLO QCD evolution (the lhaid in LHAPDF6 [53] for this set is 260000) and strong coupling constant $\alpha_\text{s}(M_\text{Z}) = 0.118$. Since the employed PDF set has no photonic density, photon-induced processes are not considered. Initial-state collinear singularities are factorised with the $\overline{\text{MS}}$ scheme, consistently with what is done in NNPDF. We use the following values for the mass and width of the massive particles:

$$\begin{aligned} m_\text{t} &= 173.21\,\text{GeV}, & \Gamma_\text{t} &= 0\,\text{GeV}, \\ M_\text{Z}^\text{OS} &= 91.1876\,\text{GeV}, & \Gamma_\text{Z}^\text{OS} &= 2.4952\,\text{GeV}, \\ M_\text{W}^\text{OS} &= 80.385\,\text{GeV}, & \Gamma_\text{W}^\text{OS} &= 2.085\,\text{GeV}, \\ M_\text{H} &= 125.0\,\text{GeV}, & \Gamma_\text{H} &= 4.07 \times 10^{-3}\,\text{GeV}, \end{aligned} \tag{2}$$

and renormalise the EW coupling in the G_μ scheme [54] where

$$G_\mu = 1.16637 \times 10^{-5}\,\text{GeV}^{-2}. \tag{3}$$

The derived value of the EW coupling α, corresponding to our choice of input parameters, is

$$\alpha = 7.555310522369 \times 10^{-3}. \tag{4}$$

We employ the complex-mass scheme [55, 56] to treat unstable intermediate particles in a gauge-invariant manner CHECK THAT ALL CODES USE THE CMS.

The renormalisation and factorisation scales are set dynamically as

$$\mu_\text{ren} = \mu_\text{fac} = \sqrt{p_{\text{T,j}_1}\, p_{\text{T,j}_2}}, \tag{5}$$

Cross sections and distribution are computed within the following VBS cuts inspired from experimental measurements [1, 4, 2, 57]:

– The two same-sign charged leptons are required to have

$$p_{\text{T},\ell} > 20\,\text{GeV}, \qquad |y_\ell| < 2.5, \qquad \Delta R_{\ell\ell} > 0.3\,. \tag{6}$$

– The total missing transverse energy, computed from the vectorial sum of the transverse momenta of the two neutrinos in the event, is required to be

$$E_{\text{T,miss}} = p_{\text{T,miss}} > 40\,\text{GeV}\,. \tag{7}$$

– QCD partons (quarks and gluons) are clustered together using the anti-k_T algorithm [58] with distance parameter $R = 0.4$. Jets are required to have

$$p_{\text{T,j}} > 30\,\text{GeV}, \qquad |y_\text{j}| < 4.5, \qquad \Delta R_{\text{j}\ell} > 0.3\,. \tag{8}$$

On the two jets with largest transverse-momentum the following invariant-mass and rapidity-separation cuts are imposed

$$m_\text{jj} > 500\,\text{GeV}, \qquad |\Delta y_\text{jj}| > 2.5. \tag{9}$$

– When EW corrections are computed, real photons and charged fermion are clustered together using the anti-k_T algorithm with radius parameter $R = 0.1$. In this case, leptons and quarks mentioned above must be understood as dressed fermions. Photons which are not combined at this step are clustered with QCD partons to form jets as it is described previously.

4 Leading-order study

4.1 Three contributions

At tree level, there are three contributions to the W^+W^+ production in association with two jets: the pure EW component $\mathcal{O}(\alpha^6)$, the interference $\mathcal{O}(\alpha_\text{s}\alpha^5)$ and the QCD background $\mathcal{O}(\alpha_\text{s}^2\alpha^4)$.
The three contributions to the jet–jet invariant mass M_{jj} and positive rapidity difference $|\Delta y_{jj}|$ distributions are shown in Fig. 2, together with their sum. Concerning the QCD contribution, it is worth noticing that for quantum number conservation external gluons cannot contribute at LO, thus the $\mathcal{O}(\alpha_\text{s}^2\alpha^4)$ diagrams only involve t/u–channel virtual gluons: this results in a small QCD background, although the VBF topological cuts are not imposed. The interference between EW and QCD contributions is small, due to color suppression, but not negligible (t/u interference with identical fermions). The LO cross–section for the three perturbative orders are shown in table 2. The EW, QCD and interference amount respectively to 57%, 37% and 6% of the total inclusive cross section. In the presence of typical VBS cuts, the EW contribution

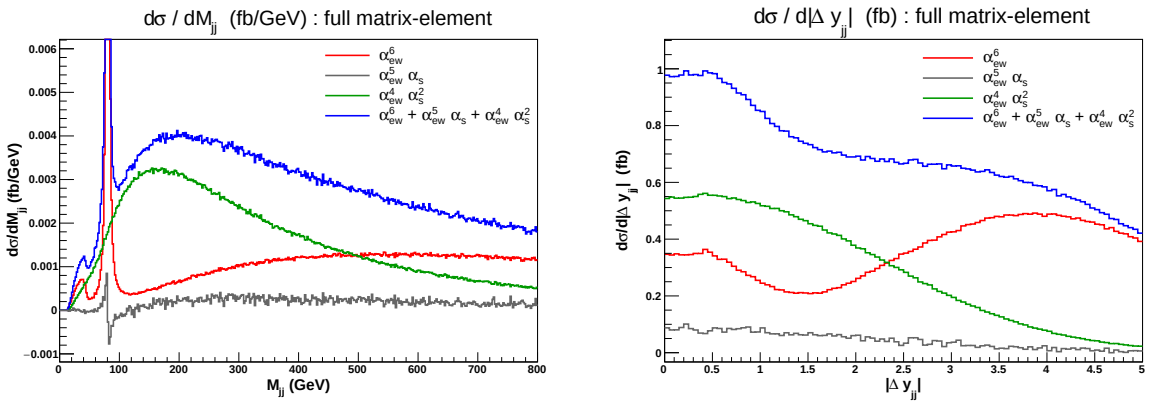

Fig. 2: Differential distribution in the jet–jet invariant mass M_{jj} (left) and the positive difference of the jet rapidities $|\Delta y_{jj}|$ (right) at LO. EW contribution in red, QCD in green, interference in gray and sum in blue. No cuts on M_{jj} and $|\Delta y_{jj}|$ are applied. Results of full LO matrix element simulation.

Code	σ[fb]($\mathcal{O}(\alpha^6)$)	σ[fb]($\mathcal{O}(\alpha_s^2\alpha^4)$)	σ[fb]($\mathcal{O}(\alpha_s\alpha^5)$)
Phantom	2.292 ± 0.002	1.477 ± 0.001	0.223 ± 0.003
Xxx	$\pm$	$\pm$	$\pm$

Table 2: Cross sections at LO accuracy for the pp $\to \mu^+\nu_\mu e^+\nu_e jj$ process: these results concern the setup described in section 3.3, apart from the M_{jj} and $|\Delta y_{jj}|$ cuts which have been dropped.

is strongly enhanced, as shown in section 4.3.
The EW contribution to the M_{jj} distribution (red curve in Fig. 2) shows a huge peak around the W mass: this is due to the possibility for the two jets to be decay products of a W^- boson. Note that this effect doesn't arise in calculations which employ VBS approximation (see VBS approx. description in section [ref.]). One can also see this in three different plots in the plan $(m_{jj}, \Delta y_{jj})$.

4.2 Inclusive comparison

4.3 Comparison in the fiducial region

In Tab. 3 we report the total rates at LO accuracy obtained with the set-up described above, and in Fig. 5 we show the results for the tagging-jet (left) and lepton-pair (right) invariant-mass distribution. In both cases we show the absolute distributions in the main frame of the figures, while in the inset the ratio over VBFNLO is displayed. For both observables we find an excellent agreement among the various tools, which confirms the fact that contributions from $s-$channel diagrams as well as from non-resonant configurations are strongly suppressed in the fiducial region. We have checked that the same level of agreement holds for many other differential distributions.

Code	σ[fb]
Bonsay	$X \pm 0.0002$
MG5_aMC	$X \pm 0.001$
MoCaNLO+Recola	1.4347 ± 0.0001
PHANTOM	1.4374 ± 0.0006
POWHEG	1.44092 ± 0.00009
VBFNLO	1.43796 ± 0.00005
Whizard	1.4360 ± 0.0005

Table 3: Rates at LO accuracy within VBS cuts obtained with the different codes used in this comparison, for the pp $\to \mu^+\nu_\mu e^+\nu_e jj$ process.

5 Next-to-leading order QCD

5.1 Inclusive comparision

Scan at NLO

5.2 Comparison in the fiducial region

Cross secitons at NLO

At NLO, rates show slightly larger discrepancies, as it can be observed in Tab. 5. This is most likely due to low dijet invariant-mass configurations, where $s-$channel diagrams and interferences are less suppressed than at LO, because of the presence of extra QCD radiation.

Distributions at NLO

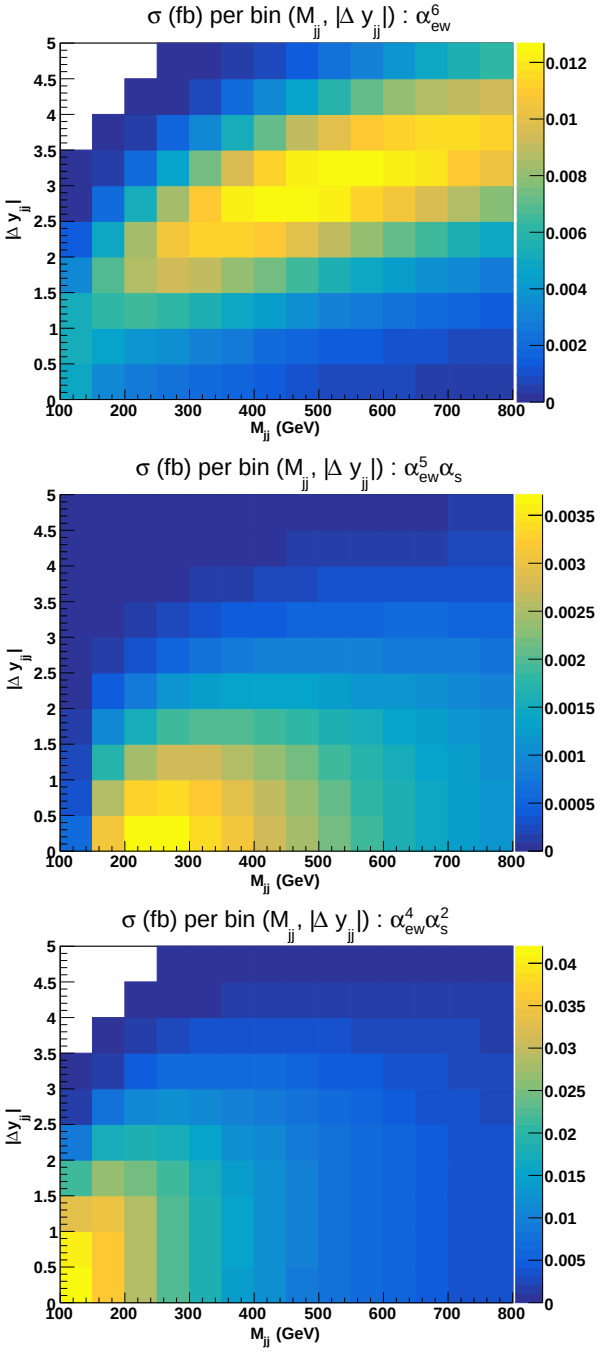

Fig. 3: Cross sections (fb) per bin in the plan $(m_{\rm jj}, \Delta y_{\rm jj})$ for the three LO contributions of orders $\mathcal{O}(\alpha^6)$ (top left), $\mathcal{O}(\alpha^5\alpha_{\rm s})$ (top right), and $\mathcal{O}(\alpha^4\alpha_{\rm s}^2)$ (bottom).

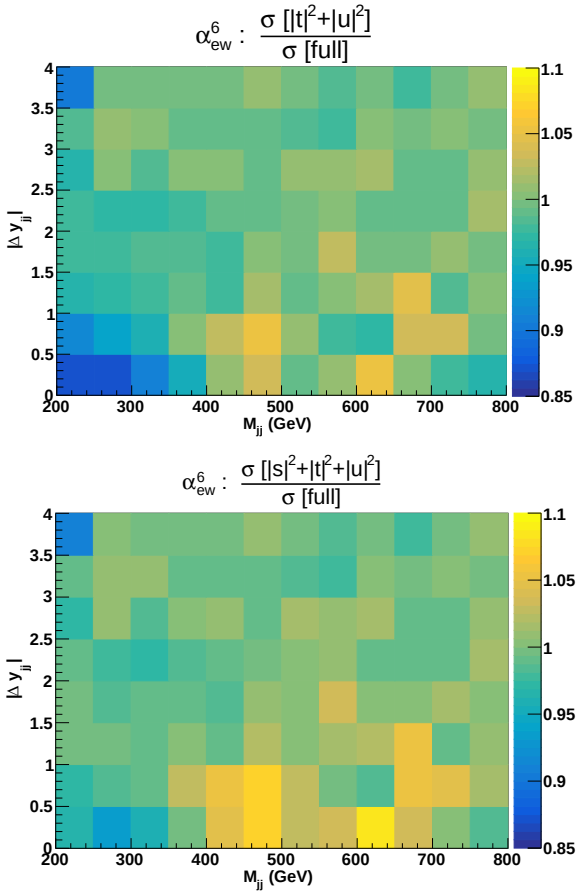

Fig. 4: Cross sections (fb) per bin in the plan $(m_{\rm jj}, \Delta y_{\rm jj})$ at order $\mathcal{O}(\alpha^6)$. Ratio of approximated squared amplitudes over the full matrix element. The approximated squared amplitudes are computed as $|\mathcal{A}|^2 \sim |t|^2 + |u|^2$ (left) and $|\mathcal{A}|^2 \sim |s|^2 + |t|^2 + |u|^2$ (right).

Code	σ[fb]
Bonsay	$X \pm 0.0009$
MG5_aMC	$X \pm 0.003$
MoCaNLO+Recola	1.382 ± 0.002
POWHEG	1.3556 ± 0.0009
VBFNLO	1.3916 ± 0.0001

Table 4: Rates at NLO-QCD accuracy within VBS cuts obtained with the different codes used in this comparison, for the $\rm pp \to \mu^+\nu_\mu e^+\nu_e jj$ process.

6 Matching to parton shower

We now turn to discuss how different predictions compare when the matching to parton-shower (PS) is included. For such a comparison we expect larger discrepancy than what we found at fixed-order, as a consequence of the different matching schemes, PS employed and of the other details of the matching (such as the choice of the shower initial scale). Among the codes capable of providing fixed-order results, presented before, MG5_aMC, POWHEG and VBFNLO can also provide results at (N)LO+PS accuracy. Besides, also PHANTOM is employed for LO+PS results.

MG5_aMC, which employs the MC@NLO [59] matching

procedure, will be used together with Pythia8 [60] (version 2.2.3) and Herwig++ [61, 62] (version 2.7.1). For POWHEG, the omonymous matching procedure is employed [63, 44], together with Pythia8 MZ VERSION? if same as MG5, put it at the end together with the tune. VBFNLO makes it possible to choose between the MC@NLO and POWHEG matching, in both cases together with Herwig7 []. Finally, PHANTOM results will be shown matched with Pythia 8. Whenever Pythia8 is used, the Monash tune [64] is selected.

Results will be presented within the cuts described in Section 3.3, applied after shower and hadronization (this implies that jets are obtained by clustering stable hadrons, and not QCD partons). This implies that at the event-generation level, looser cuts (or no cuts at all) must be employed in order not to bias the results. MZ lepton-jet separation at the hard-event level?.

A slightly different setup has been employed for MG5_aMC in order to simplify the calculation: instead of generating the full pp $\to \mu^+\nu_\mu e^+\nu_e jj$ process, since it is anyway dominated by doubly-resonant contribution, the events are produced for the process with two stable W^+ bosons (pp $\to W^+W^+jj$), and these W^+ bosons are decayed with MadSpin [65] (keeping spin correlations) before the PS. Since MadSpin computes the partial and total decay width of the W bosons at LO accuracy only, while in Section 3.3 the NLO width is employed, a small effect (6%) on the normalisation of distribution is induced. Finally, when the renormalisation and factorisation scales are set, the $\Delta R_{j\ell}$ cut is not imposed during the jet-clustering procedure, but this has no visible effect on the results.

We now turn to present the results:

Code	σ[fb]
MG5_aMC+Pythia8	$1.450(1.368) \pm 0.$
MG5_aMC+Herwig++	$1.445(1.363) \pm 0.$
POWHEG	1.3633 ± 0.0004
VBFNLO	$1.339 \pm 0.$
MG5_aMC+Pythia8 (LO)	$1.352(1.275) \pm 0.$
MG5_aMC+Herwig++ (LO)	$1.343(1.267) \pm 0.$
PHANTOM+Pythia8	$1.235 \pm 0.$

Table 5: Rates at NLO-QCD (LO-QCD) accuracy matched to parton shower within VBS cuts obtained with the different codes used in this comparison, for the pp $\to \mu^+\nu_\mu e^+\nu_e jj$ process. Numbers in parentheses for the MG5_aMC simulations are rescaled to account for the effect related to the boson widths computed by MadSpin, see the text for details.

MZ: MC uncertainties???

7 Conclusion

- Sum-up of the study.

[MP: This might deserve a section on its own.]

Recommendations to experimental collaborations:
- Combinations with EW NLO corrections.
- Missing higher EW order: $\pm\delta^2_{\rm NLOEW}$
- Systematics when using NLO QCD approximation
- Systematics of different parton shower
- Combined measurement including EW, QCD, and interference
- Move to NLO predictions / generators
- Comment on the irreducible QCD background

Acknowledgements

We thank ... Acknowledgement of VBSCAN COST action.

Appendix A: Appendix one

References

1. ATLAS Collaboration, G. Aad et al., Evidence for Electroweak Production of $W^\pm W^\pm jj$ in pp Collisions at $\sqrt{s} = 8$ TeV with the ATLAS Detector. Phys. Rev. Lett. 113 (2014) no. 14, 141803, arXiv:1405.6241 [hep-ex].
2. CMS Collaboration, V. Khachatryan et al., Study of vector boson scattering and search for new physics in events with two same-sign leptons and two jets. Phys. Rev. Lett. 114 (2015) no. 5, 051801, arXiv:1410.6315 [hep-ex].
3. CMS Collaboration, A. M. Sirunyan et al., Observation of electroweak production of same-sign W boson pairs in the two jet and two same-sign lepton final state in proton-proton collisions at $\sqrt{s} = 13$ TeV. arXiv:1709.05822 [hep-ex].
4. ATLAS Collaboration, M. Aaboud et al., Measurement of $W^\pm W^\pm$ vector-boson scattering and limits on anomalous quartic gauge couplings with the ATLAS detector. Phys. Rev. D96 (2017) 012007, arXiv:1611.02428 [hep-ex].
5. B. Jäger, C. Oleari, and D. Zeppenfeld, Next-to-leading order QCD corrections to W^+W^+jj and W^-W^-jj production via weak-boson fusion. Phys. Rev. D80 (2009) 034022, arXiv:0907.0580 [hep-ph].

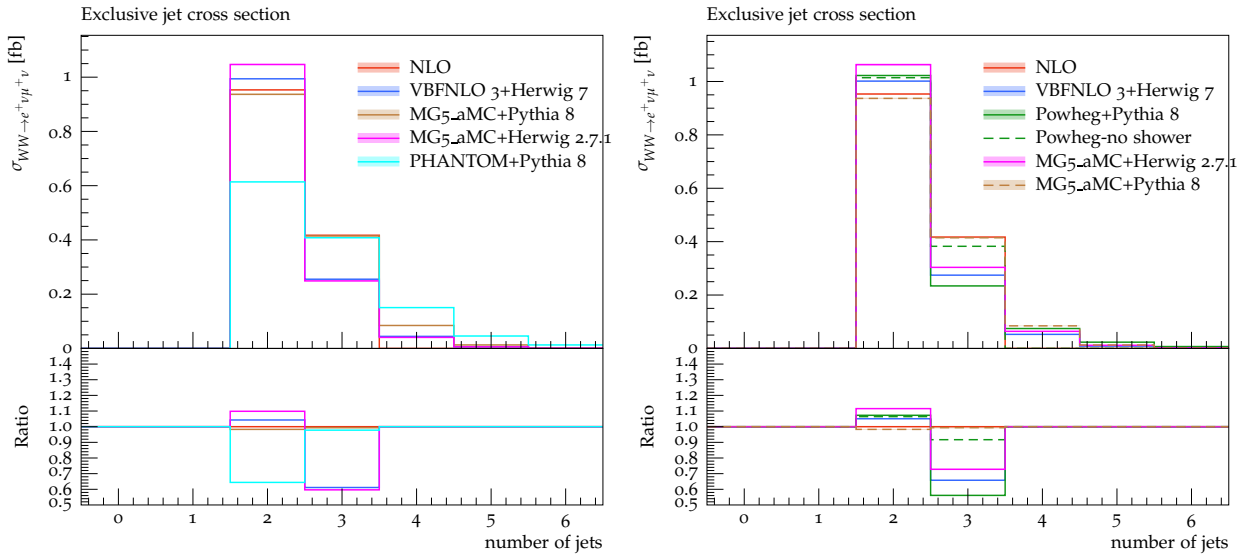

Fig. 8: Exclusive jet multiplicity from predictions matched to parton shower, at LO (left) or NLO (right) accuracy, compared with the fixed-NLO result computed with VBFNLO

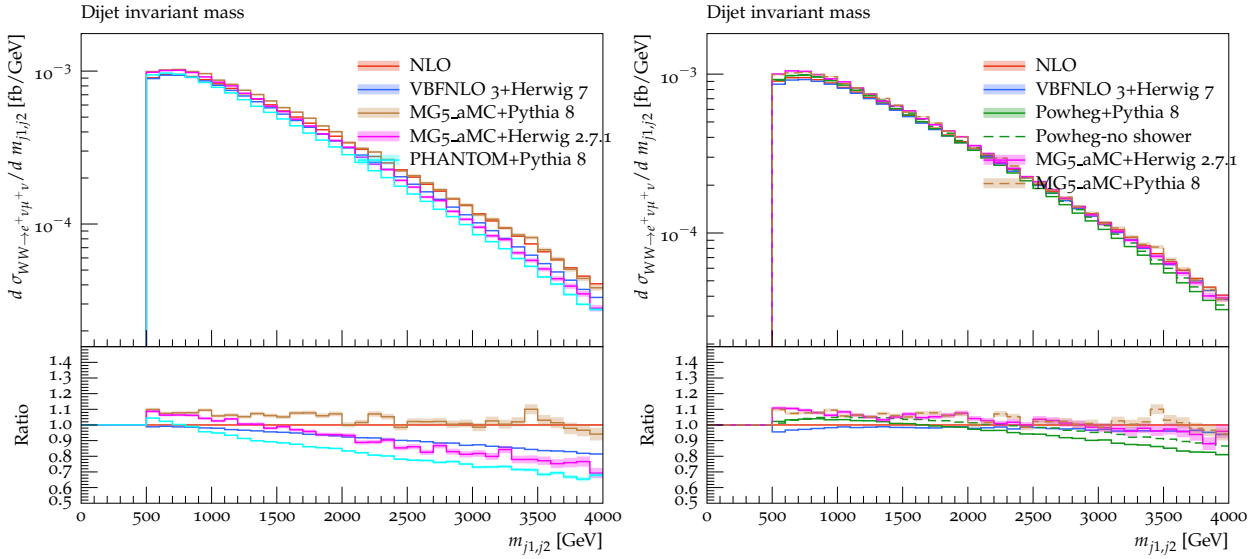

Fig. 9: Same as in Fig. 8, for the invariant mass of the two tagging jets.

6. B. Jäger and G. Zanderighi, NLO corrections to electroweak and QCD production of W^+W^+ plus two jets in the POWHEGBOX. JHEP 11 (2011) 055, arXiv:1108.0864 [hep-ph].
7. A. Denner, L. Hošeková, and S. Kallweit, NLO QCD corrections to W^+W^+jj production in vector-boson fusion at the LHC. Phys. Rev. D86 (2012) 114014, arXiv:1209.2389 [hep-ph].
8. M. Rauch, Vector-Boson Fusion and Vector-Boson Scattering. arXiv:1610.08420 [hep-ph].
9. T. Melia, K. Melnikov, R. Röntsch, and G. Zanderighi, Next-to-leading order QCD predictions for W^+W^+jj production at the LHC. JHEP 12 (2010) 053, arXiv:1007.5313 [hep-ph].
10. T. Melia, P. Nason, R. Röntsch, and G. Zanderighi, W^+W^+ plus dijet production in the POWHEGBOX. Eur. Phys. J. C71 (2011) 1670, arXiv:1102.4846 [hep-ph].
11. F. Campanario, M. Kerner, L. D. Ninh, and D. Zeppenfeld, Next-to-leading order QCD corrections to W^+W^+ and W^-W^- production in association with two jets. Phys. Rev. D89 (2014) no. 5, 054009, arXiv:1311.6738 [hep-ph].

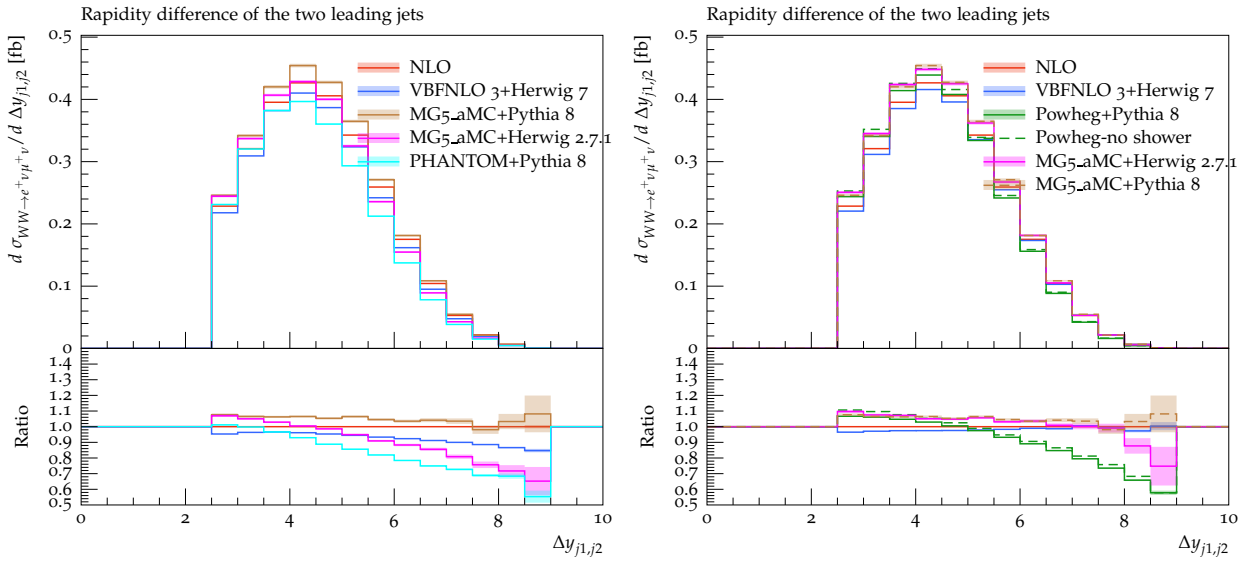

Fig. 10: Same as in Fig. 8, for the rapidity separation of the two tagging jets.

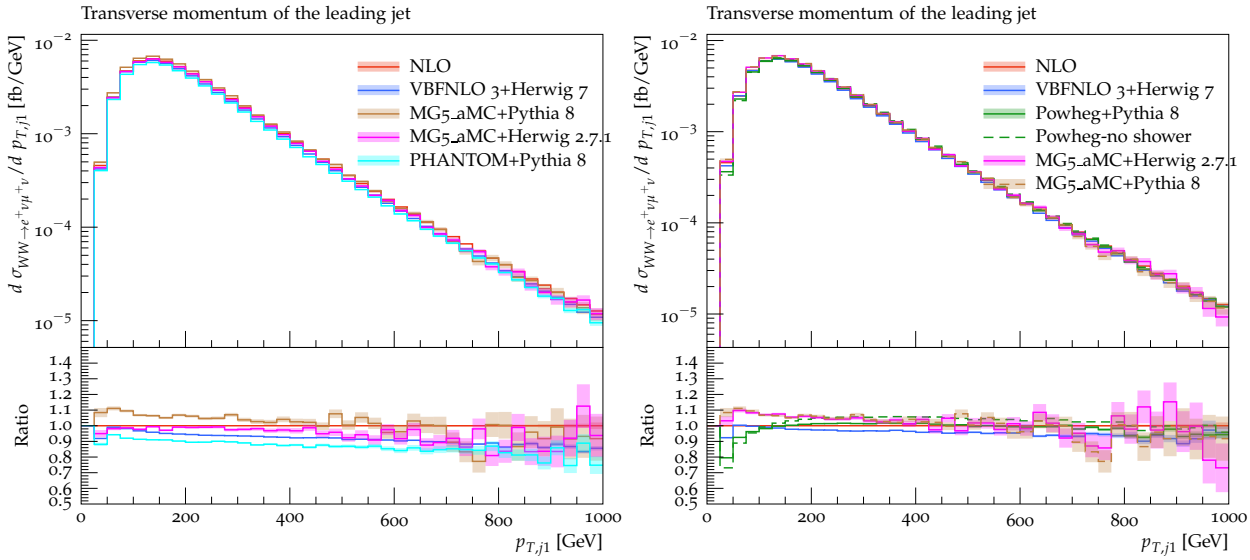

Fig. 11: Same as in Fig. 8, for the transverse momentum of the hardest jet.

12. J. Baglio et al., Release Note - VBFNLO 2.7.0. arXiv:1404.3940 [hep-ph].
13. B. Biedermann, A. Denner, and M. Pellen, Complete NLO corrections to W^+W^+ scattering and its irreducible background at the LHC. arXiv:1708.00268 [hep-ph].
14. B. Biedermann, A. Denner, and M. Pellen, Large electroweak corrections to vector-boson scattering at the Large Hadron Collider. Phys. Rev. Lett. 118 (2017) no. 26, 261801, arXiv:1611.02951 [hep-ph].
15. I. Kuss and H. Spiesberger, Luminosities for vector boson - vector boson scattering at high-energy colliders. Phys. Rev. D53 (1996) 6078–6093, arXiv:hep-ph/9507204 [hep-ph].
16. E. Accomando, A. Denner, and S. Pozzorini, Logarithmic electroweak corrections to $e^+e^- \to \nu_e\bar{\nu}_e W^+W^-$. JHEP 03 (2007) 078, arXiv:hep-ph/0611289 [hep-ph].
17. S. Dittmaier and C. Schwan, Non-factorizable photonic corrections to resonant production and decay of many unstable particles. Eur. Phys. J. C76 (2016) no. 3, 144, arXiv:1511.01698 [hep-ph].
18. S. Dittmaier and M. Roth, LUSIFER: A LUcid approach to six FERmion production. Nucl. Phys. B642 (2002) 307–343, arXiv:hep-ph/0206070 [hep-ph].

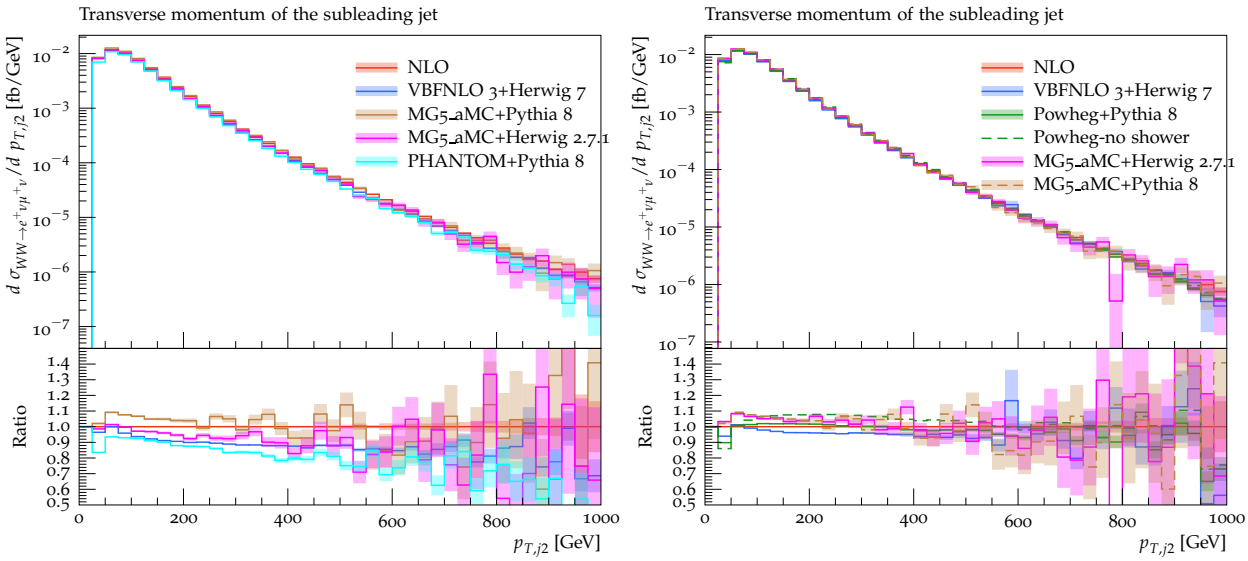

Fig. 12: Same as in Fig. 8, for the transverse momentum of the second-hardest jet.

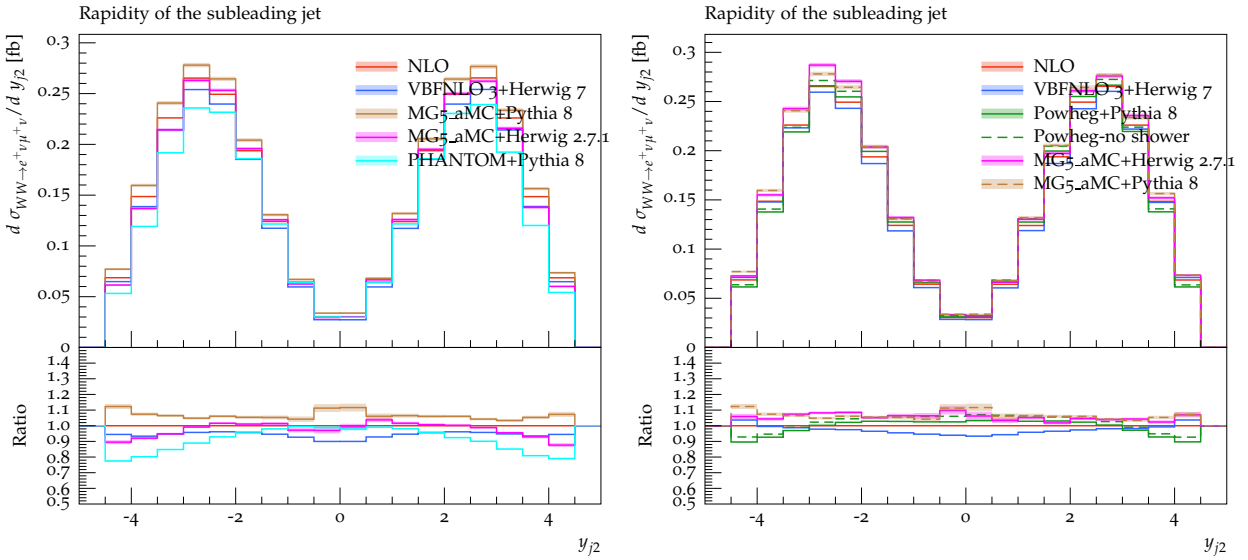

Fig. 13: Same as in Fig. 8, for the rapidity of the second-hardest jet.

19. A. Denner, S. Dittmaier, and L. Hofer, COLLIER - A fortran-library for one-loop integrals. PoS LL2014 (2014) 071, arXiv:1407.0087 [hep-ph].
20. A. Denner, S. Dittmaier, and L. Hofer, Collier: a fortran-based Complex One-Loop LIbrary in Extended Regularizations. Comput. Phys. Commun. 212 (2017) 220–238, arXiv:1604.06792 [hep-ph].
21. J. Alwall et al., The automated computation of tree-level and next-to-leading order differential cross sections, and their matching to parton shower simulations. JHEP 07 (2014) 079, arXiv:1405.0301 [hep-ph].
22. S. Frixione, Z. Kunszt, and A. Signer, Three jet cross-sections to next-to-leading order. Nucl. Phys. B467 (1996) 399–442, arXiv:hep-ph/9512328 [hep-ph].
23. S. Frixione, A General approach to jet cross-sections in QCD. Nucl. Phys. B507 (1997) 295–314, arXiv:hep-ph/9706545 [hep-ph].
24. R. Frederix, S. Frixione, F. Maltoni, and T. Stelzer, Automation of next-to-leading order computations in QCD: The FKS subtraction. JHEP 10 (2009) 003, arXiv:0908.4272 [hep-ph].
25. R. Frederix, S. Frixione, A. S. Papanastasiou, S. Prestel, and P. Torrielli, Off-shell single-top

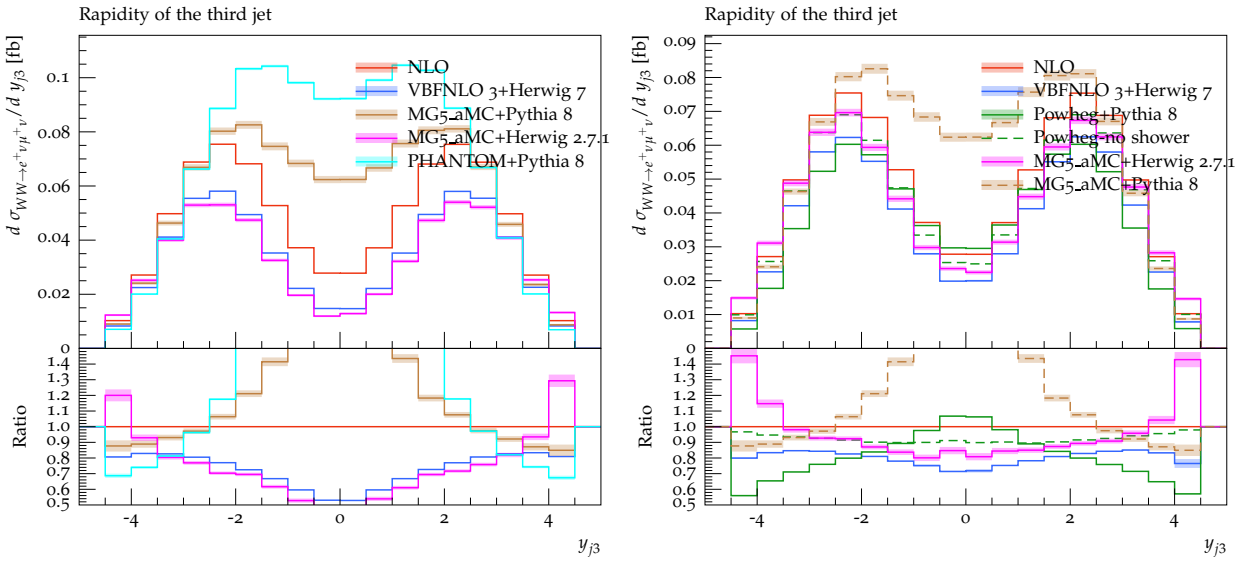

Fig. 14: Same as in Fig. 8, for the rapidity of the third-hardest jet.

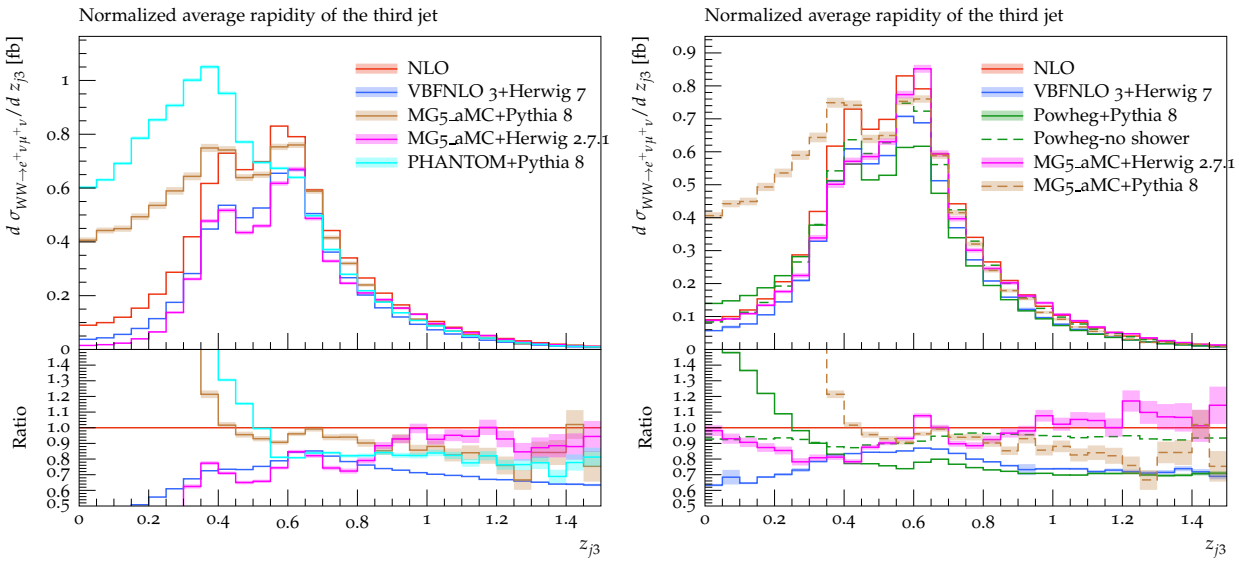

Fig. 15: Same as in Fig. 8, for the z variable of the third-hardest jet.

production at NLO matched to parton showers. JHEP 06 (2016) 027, arXiv:1603.01178 [hep-ph].

26. G. Ossola, C. G. Papadopoulos, and R. Pittau, Reducing full one-loop amplitudes to scalar integrals at the integrand level. Nucl. Phys. B763 (2007) 147–169, arXiv:hep-ph/0609007 [hep-ph].
27. P. Mastrolia, E. Mirabella, and T. Peraro, Integrand reduction of one-loop scattering amplitudes through Laurent series expansion. JHEP 06 (2012) 095, arXiv:1203.0291 [hep-ph]. [Erratum: JHEP11,128(2012)].
28. G. Passarino and M. J. G. Veltman, One-loop corrections for e^+e^- annihilation into $\mu^+\mu^-$ in the Weinberg model. Nucl. Phys. B160 (1979) 151–207.
29. A. I. Davydychev, A Simple formula for reducing Feynman diagrams to scalar integrals. Phys. Lett. B263 (1991) 107–111.
30. A. Denner and S. Dittmaier, Reduction schemes for one-loop tensor integrals. Nucl. Phys. B734 (2006) 62–115, hep-ph/0509141.
31. V. Hirschi, R. Frederix, S. Frixione, M. V. Garzelli, F. Maltoni, and R. Pittau, Automation of one-loop QCD corrections. JHEP 05 (2011) 044, arXiv:1103.0621 [hep-ph].

32. G. Ossola, C. G. Papadopoulos, and R. Pittau, CutTools: A Program implementing the OPP reduction method to compute one-loop amplitudes. JHEP 03 (2008) 042, arXiv:0711.3596 [hep-ph].
33. T. Peraro, Ninja: Automated Integrand Reduction via Laurent Expansion for One-Loop Amplitudes. Comput. Phys. Commun. 185 (2014) 2771–2797, arXiv:1403.1229 [hep-ph].
34. V. Hirschi and T. Peraro, Tensor integrand reduction via Laurent expansion. JHEP 06 (2016) 060, arXiv:1604.01363 [hep-ph].
35. H.-S. Shao, Iregi user manual, unpublished.
36. F. Cascioli, P. Maierhöfer, and S. Pozzorini, Scattering Amplitudes with Open Loops. Phys. Rev. Lett. 108 (2012) 111601, arXiv:1111.5206 [hep-ph].
37. A. Ballestrero, A. Belhouari, G. Bevilacqua, V. Kashkan, and E. Maina, PHANTOM: A Monte Carlo event generator for six parton final states at high energy colliders. Comput. Phys. Commun. 180 (2009) 401–417, arXiv:0801.3359 [hep-ph].
38. A. Denner and S. Dittmaier, The Complex-mass scheme for perturbative calculations with unstable particles. Nucl. Phys. Proc. Suppl. 160 (2006) 22–26, arXiv:hep-ph/0605312 [hep-ph]. [,22(2006)].
39. A. Ballestrero, "PHACT: Helicity amplitudes for present and future colliders," in High energy physics and quantum field theory. Proceedings, 14th International Workshop, QFTHEP'99, Moscow, Russia, May 27-June 2, 1999, pp. 303–309. 1999. arXiv:hep-ph/9911318 [hep-ph].
40. A. Ballestrero and E. Maina, A New method for helicity calculations. Phys. Lett. B350 (1995) 225–233, arXiv:hep-ph/9403244 [hep-ph].
41. F. Berends, P. Daverveldt, and R. Kleiss, Complete lowest-order calculations for four-lepton final states in electron-positron collisions. Nuclear Physics B 253 (1985) no. Supplement C, 441 – 463. http://www.sciencedirect.com/science/article/pii/0550321385905413.
42. G. P. Lepage, A new algorithm for adaptive multidimensional integration. Journal of Computational Physics 27 (1978) no. 2, 192 – 203. http://www.sciencedirect.com/science/article/pii/0021999178900049.
43. S. Alioli, P. Nason, C. Oleari, and E. Re, A general framework for implementing NLO calculations in shower Monte Carlo programs: the POWHEG BOX. JHEP 06 (2010) 043, arXiv:1002.2581 [hep-ph].
44. S. Frixione, P. Nason, and C. Oleari, Matching NLO QCD computations with Parton Shower simulations: the POWHEG method. JHEP 11 (2007) 070, arXiv:0709.2092 [hep-ph].
45. K. Arnold et al., VBFNLO: A Parton level Monte Carlo for processes with electroweak bosons. Comput. Phys. Commun. 180 (2009) 1661–1670, arXiv:0811.4559 [hep-ph].
46. K. Arnold et al., VBFNLO: A Parton Level Monte Carlo for Processes with Electroweak Bosons – Manual for Version 2.5.0. arXiv:1107.4038 [hep-ph].
47. R. Feger, "MoCaNLO: a generic Monte Carlo event generator for NLO calculations of hadron-collider processes." unpublished, 2015.
48. S. Actis et al., Recursive generation of one-loop amplitudes in the Standard Model. JHEP 04 (2013) 037, arXiv:1211.6316 [hep-ph].
49. S. Actis et al., RECOLA: REcursive Computation of One-Loop Amplitudes. Comput. Phys. Commun. 214 (2017) 140–173, arXiv:1605.01090 [hep-ph].
50. M. Moretti, T. Ohl, and J. Reuter, O'Mega: An Optimizing matrix element generator. arXiv:hep-ph/0102195 [hep-ph].
51. W. Kilian, T. Ohl, and J. Reuter, WHIZARD: Simulating Multi-Particle Processes at LHC and ILC. Eur. Phys. J. C71 (2011) 1742, arXiv:0708.4233 [hep-ph].
52. NNPDF Collaboration, R. D. Ball et al., Parton distributions for the LHC Run II. JHEP 04 (2015) 040, arXiv:1410.8849 [hep-ph].
53. A. Buckley, J. Ferrando, S. Lloyd, K. Nordström, B. Page, M. Rüfenacht, M. Schönherr, and G. Watt, LHAPDF6: parton density access in the LHC precision era. Eur. Phys. J. C75 (2015) 132, arXiv:1412.7420 [hep-ph].
54. A. Denner, S. Dittmaier, M. Roth, and D. Wackeroth, Electroweak radiative corrections to $e^+e^- \to WW \to 4$ fermions in double-pole approximation: The RACOONWW approach. Nucl. Phys. B587 (2000) 67–117, arXiv:hep-ph/0006307 [hep-ph].
55. A. Denner et al., Predictions for all processes $e^+e^- \to 4\text{fermions} + \gamma$. Nucl. Phys. B560 (1999) 33–65, arXiv:hep-ph/9904472.
56. A. Denner et al., Electroweak corrections to charged-current $e^+e^- \to 4$ fermion processes: Technical details and further results. Nucl. Phys. B724 (2005) 247–294, arXiv:hep-ph/0505042.
57. CMS Collaboration, Observation of electroweak production of same-sign W boson pairs in the two jet and two same-sign lepton final state in

proton-proton collisions at 13 TeV. CMS-PAS-SMP-17-004.
58. M. Cacciari, G. P. Salam, and G. Soyez, The anti-k_t jet clustering algorithm. JHEP 04 (2008) 063, arXiv:0802.1189 [hep-ph].
59. S. Frixione and B. R. Webber, Matching NLO QCD computations and parton shower simulations. JHEP 06 (2002) 029, arXiv:hep-ph/0204244 [hep-ph].
60. T. Sjöstrand, S. Ask, J. R. Christiansen, R. Corke, N. Desai, P. Ilten, S. Mrenna, S. Prestel, C. O. Rasmussen, and P. Z. Skands, An Introduction to PYTHIA 8.2. Comput. Phys. Commun. 191 (2015) 159–177, arXiv:1410.3012 [hep-ph].
61. M. Bahr et al., Herwig++ Physics and Manual. Eur. Phys. J. C58 (2008) 639–707, arXiv:0803.0883 [hep-ph].
62. J. Bellm et al., Herwig++ 2.7 Release Note. arXiv:1310.6877 [hep-ph].
63. P. Nason, A New method for combining NLO QCD with shower Monte Carlo algorithms. JHEP 11 (2004) 040, arXiv:hep-ph/0409146 [hep-ph].
64. P. Skands, S. Carrazza, and J. Rojo, Tuning PYTHIA 8.1: the Monash 2013 Tune. Eur. Phys. J. C74 (2014) no. 8, 3024, arXiv:1404.5630 [hep-ph].
65. P. Artoisenet, R. Frederix, O. Mattelaer, and R. Rietkerk, Automatic spin-entangled decays of heavy resonances in Monte Carlo simulations. JHEP 03 (2013) 015, arXiv:1212.3460 [hep-ph].

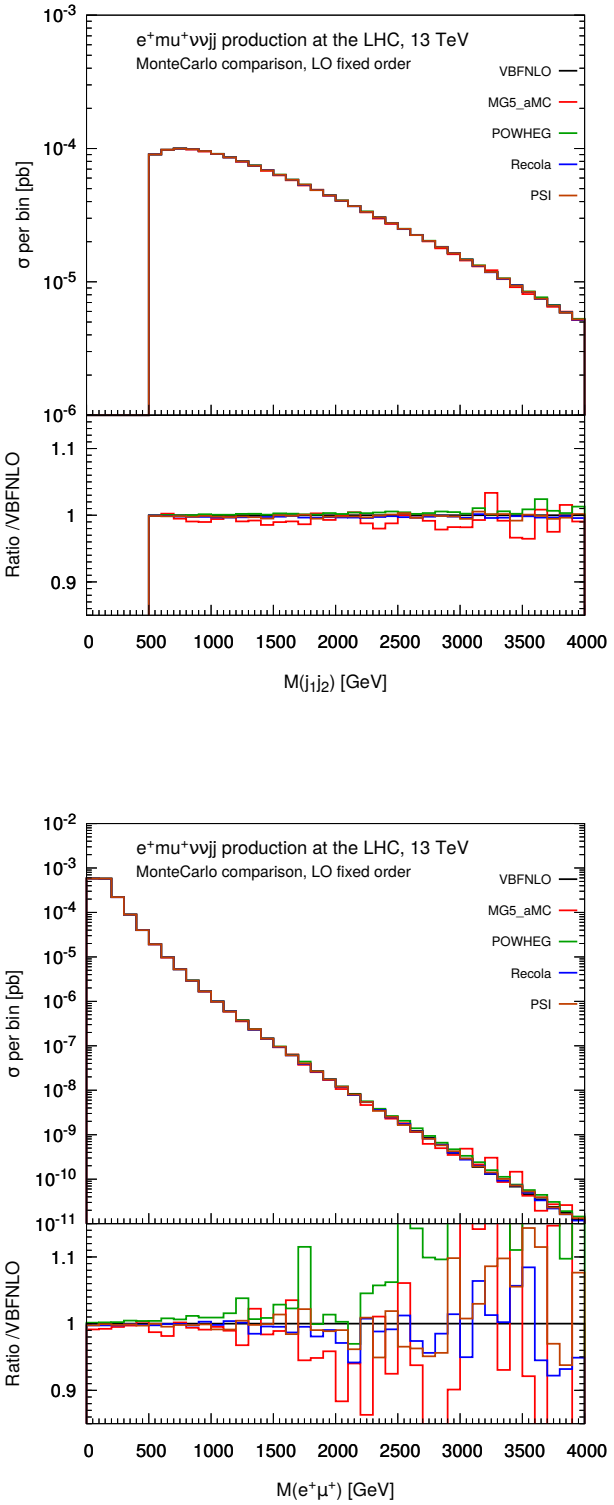

Fig. 5: Invariant-mass of the two tagging jets (left) and of the two leptons (right), at LO accuracy, computed with the different codes used in this comparison. The inset shows the ratio over VBFNLO.

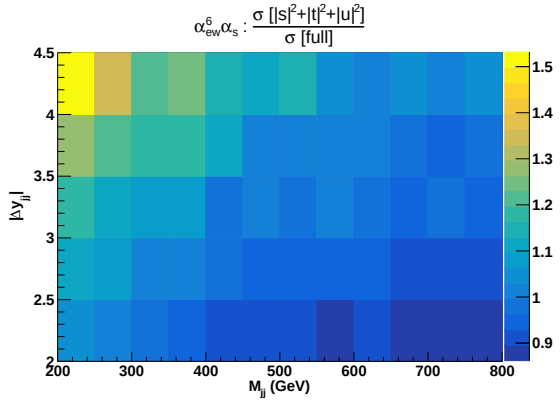

FIGURE

Fig. 6: Cross section (fb) per bin of (M_{jj}, Δy_{jj}) at NLO QCD $\mathcal{O}(\alpha^6\alpha_s)$, without any cut on the jj pair kinematics: ratio of approximated squared amplitudes over the full matrix element. The approximated squared amplitudes are computed as $|\mathcal{A}|^2 \sim |s|^2 + |t|^2 + |u|^2$. Results of VBFNLO (approximated) and RECOLA (full) calculations.

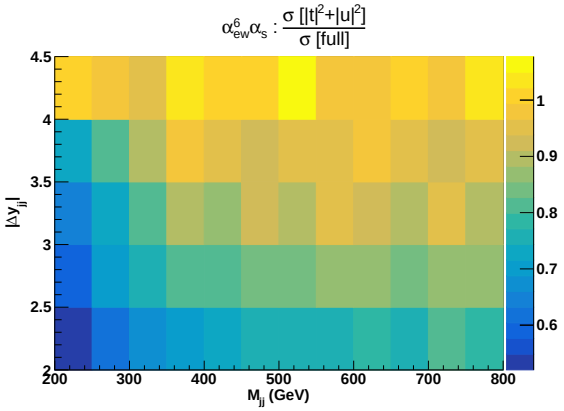

Fig. 7: Cross sections (fb) per bin of (M_{jj}, Δy_{jj}) at NLO QCD $\mathcal{O}(\alpha^6\alpha_s)$, without any cut on the jj pair kinematics: ratio of approximated squared amplitudes over the full matrix element. The approximated squared amplitudes are computed as $|\mathcal{A}|^2 \sim |t|^2 + |u|^2$. Results of VBFNLO (approximated) and RECOLA (full) calculations.